

RNF8 Ubiquitylates Histones at DNA Double-Strand Breaks and Promotes Assembly of Repair Proteins

Niels Mailand,^{1,2} Simon Bekker-Jensen,^{1,2} Helene Faustrup,¹ Fredrik Melander,¹ Jiri Bartek,¹ Claudia Lukas,¹ and Jiri Lukas^{1,*}

¹Institute of Cancer Biology and Centre for Genotoxic Stress Research, Danish Cancer Society, Strandboulevarden 49, DK-2100, Copenhagen, Denmark

²These authors contributed equally to this work.

*Correspondence: jil@cancer.dk

DOI 10.1016/j.cell.2007.09.040

SUMMARY

Accumulation of repair proteins on damaged chromosomes is required to restore genomic integrity. However, the mechanisms of protein retention at the most destructive chromosomal lesions, the DNA double-strand breaks (DSBs), are poorly understood. We show that RNF8, a RING-finger ubiquitin ligase, rapidly assembles at DSBs via interaction of its FHA domain with the phosphorylated adaptor protein MDC1. This is accompanied by an increase in DSB-associated ubiquitylations and followed by accumulation of 53BP1 and BRCA1 repair proteins. Knockdown of RNF8 or disruption of its FHA or RING domains impaired DSB-associated ubiquitylation and inhibited retention of 53BP1 and BRCA1 at the DSB sites. In addition, we show that RNF8 can ubiquitylate histone H2A and H2AX, and that its depletion sensitizes cells to ionizing radiation. These data suggest that MDC1-mediated and RNF8-executed histone ubiquitylation protects genome integrity by licensing the DSB-flanking chromatin to concentrate repair factors near the DNA lesions.

INTRODUCTION

Among the most prominent cytological manifestations of DNA breakage is formation of the ionizing radiation-induced foci (IRIF). These nuclear structures reflect local chromatin expansion, posttranslational modifications of histones, and assembly of diverse proteins in the vicinity of chromosomal lesions (Fernandez-Capetillo et al., 2004; Kruhlak et al., 2006). In mammals, phosphorylation of histone H2AX (γ -H2AX) by the ATM kinase is among the most proximal DSB-induced histone modifications and the prerequisite for the sustained retention of signaling

and repair proteins. Specifically, the proteins that avidly accumulate on the γ -H2AX-marked chromatin include the components of the MRE11-NBS1-RAD50 (MRN) complex, the ATM kinase, and a group of large adaptor proteins such as MDC1, 53BP1, and BRCA1 (Bekker-Jensen et al., 2006). The increased concentration of these proteins is believed to enhance the effectiveness of genome surveillance mechanisms by amplifying ATM signaling and increasing the efficiency of DSB repair (Lukas et al., 2004b).

The assembly of proteins at the DSB-flanking chromatin proceeds with distinct temporal patterns, suggesting that the formation of the DSB-induced chromatin microenvironment is a hierarchical and highly regulated process (Bekker-Jensen et al., 2005; Lukas et al., 2004a). The key interaction module engaged in direct binding to γ -H2AX resides in the BRCT domains of MDC1 (Stucki et al., 2005). MDC1 is among the first proteins to accumulate at the DSB sites (Lukas et al., 2004a), and the assembly of the γ -H2AX-MDC1 complex seems to be required for retention of most other proteins in these regions (Stucki and Jackson, 2006). Furthermore, MDC1 binding shields the C-terminal tail of γ -H2AX against premature dephosphorylation (Stewart et al., 2003; Stucki et al., 2005), a feature that helps maintain a favorable chromatin configuration until the completion of the DSB repair. Thus, MDC1 emerges as the “master regulator” determining the formation of a specific chromatin microenvironment required for genomic stability.

The way MDC1 promotes chromatin retention of other proteins involves at least two distinct mechanisms. First, there is biochemical evidence that the retention of NBS1 at the DSB-flanking chromatin is mediated by its direct interaction with MDC1 (Goldberg et al., 2003; Lukas et al., 2004a; Stewart et al., 2003). Real-time imaging of living cells supports this model by showing that MDC1 and NBS1 accumulate at the DSB-flanking chromatin very rapidly and with the same kinetics (Lukas et al., 2004a). Because NBS1 also directly binds ATM (Falck et al., 2005; You et al., 2005), the MDC1-mediated retention of NBS1 has a crucial physiological significance for the initial

stages of the DSB response as it promotes spreading of γ -H2AX from the initial breakage sites and facilitates other ATM-dependent phosphorylations (Stucki and Jackson, 2006). Second, although the retention of 53BP1 at the DSB sites is also dependent on MDC1, its accumulation at the DSB-flanking chromatin is significantly delayed (Bekker-Jensen et al., 2005). Based on this observation, and the fact that 53BP1 interacts with DSBs via binding to constitutively methylated residues on histones (Botuyan et al., 2006; Huyen et al., 2004), it has been proposed that MDC1 promotes higher-order chromatin restructuring that may increase the accessibility of histone marks. Alternatively, the formation of the γ -H2AX-MDC1 complex may promote additional modifications of the DSB-flanking chromatin that in conjunction with methylated histones increase the affinity for 53BP1.

Although intriguing, our understanding of the dynamics (and indeed the purpose) of the DSB-induced chromatin response is only rudimentary, and the above concepts leave several unanswered questions. Most notably, although it has been shown that the MDC1-NBS1 interaction requires the intact FHA domain of the latter protein (Lukas et al., 2004a), the exact structural requirements for this interaction are not understood, and whether other proteins accumulate at the DSB sites via direct binding to MDC1 has not been determined. Even more elusive are the structural and/or posttranslational events that operate between the rapid assembly of the γ -H2AX-MDC1 complexes and the delayed accumulation of 53BP1. Finally, chromatin retention of BRCA1 is also regulated by MDC1 (Bekker-Jensen et al., 2006; Lou et al., 2003) and requires at least two additional proteins, RAP80 and ABRA1 (Kim et al., 2007; Sobhian et al., 2007; Wang et al., 2007; Yan et al., 2007). However, how MDC1 functionally interacts with the RAP80-ABRA1 complex to regulate chromatin retention of BRCA1 remains an outstanding puzzle in the biology of this important tumor suppressor. In this study, we attempted to resolve these issues.

RESULTS

RNF8 Is a Novel DSB Regulator, which Binds to Chromatin in an MDC1-Dependent Manner

We performed a bioinformatic search for proteins that contain structural motifs shared by the established DSB regulators and tested their ability to accumulate at the DSB-modified chromatin. By this approach, we identified RNF8, a member of the RING-finger-containing nuclear factors (Ito et al., 2001; Plans et al., 2006), which contains a phosphothreonyl-binding FHA domain at its N terminus and a RING-finger domain at the C terminus (Figure 1A). Both domains have been previously identified in chromatin-associated DSB regulators such as NBS1 and MDC1 (the FHA domain) (Stracker et al., 2004; Stucki and Jackson, 2006) or the BRCA1-BARD1 complex (the RING domain) (Boulton, 2006). Importantly, both green fluorescence protein (GFP)-tagged RNF8 (Figures S1A and S1B) and endogenous RNF8 avidly accumulated in IRIF and in

microlaser-generated DSB tracks, respectively (Figures 1B–1E), and several pieces of evidence indicated that this DNA damage-induced accumulation reflected targeting of RNF8 to the DSB-flanking chromatin. Thus, GFP-RNF8 spanned the entire chromatin regions marked by γ -H2AX (Figure 1C, left). In addition, GFP-RNF8 accumulation at the DSBs was equally robust throughout interphase (Figure 1C, right), a feature shared by all known components of the DSB-flanking chromatin (Bekker-Jensen et al., 2006). But most significantly, the DSB-induced accumulation of RNF8 was abrogated after siRNA-mediated ablation of MDC1, the key upstream regulator of the DSB-induced chromatin response (Figure 1F). Together, these data suggest that RNF8 is a new DSB regulator that interacts with the DSB-flanking chromatin.

The FHA Domain of RNF8 Binds Phosphorylated MDC1

To elucidate how RNF8 interacts with the DSB sites, we asked whether it binds MDC1. Indeed, endogenous RNF8 and MDC1 interacted in a coimmunoprecipitation assay (Figure 2A), and we set out to explore the structural basis of this interaction. While the wild-type (WT) and RING-deficient (C403S; *RING) versions of RNF8 bound MDC1 (Figure 2B), a point mutation of a conserved residue within the FHA domain of RNF8 (R42A; *FHA) abolished the interaction (Figure 2B). Consistently, the GFP-tagged *FHA version of RNF8 failed to form nuclear foci after ionizing radiation (IR), whereas the wild-type protein or the *RING mutant avidly accumulated at DSBs (Figure 2C). We then performed a deletion analysis of the MDC1 N terminus and found that the region between amino acids 698 and 800 was necessary and sufficient for RNF8 binding (Figure S2A). This region of MDC1 contains three conserved T-Q-X-F clusters (Figure S2B) fulfilling the criteria for ATM/ATR substrates (Shiloh, 2003). While single or double substitutions of the threonine residues with alanines had little effect on binding of MDC1 to RNF8 (our unpublished data), simultaneous threonine mutations in all three clusters (designated as 3A) completely abolished this interaction (Figure 2D). To validate that the T-Q-X-F clusters could be phosphorylated *in vivo*, we exposed cells expressing the wild-type or the 3A fragments of MDC1 to IR and analyzed the immunopurified MDC1 proteins by immunoblotting with an antibody to phosphorylated SQ/TQ motifs (the consensus sites for ATM/ATR targets). Although wild-type MDC1 was phosphorylated to some extent even in nonirradiated cells (likely due to the low intrinsic ATM/ATR activity), this phosphorylation markedly increased after exposing the cells to IR, and mutation of the T-Q-X-F clusters impaired both the basal and the IR-induced phosphorylation of MDC1 (Figure 2E). Consistently, while FLAG-RNF8 and endogenous MDC1 interacted to some extent in unstressed cells, this interaction was enhanced after IR (Figure 2F). Together, these data suggest that phosphorylation of the conserved T-Q-X-F clusters of MDC1 and the integrity of the FHA domain of RNF8 are required to mediate the interaction between these two proteins.

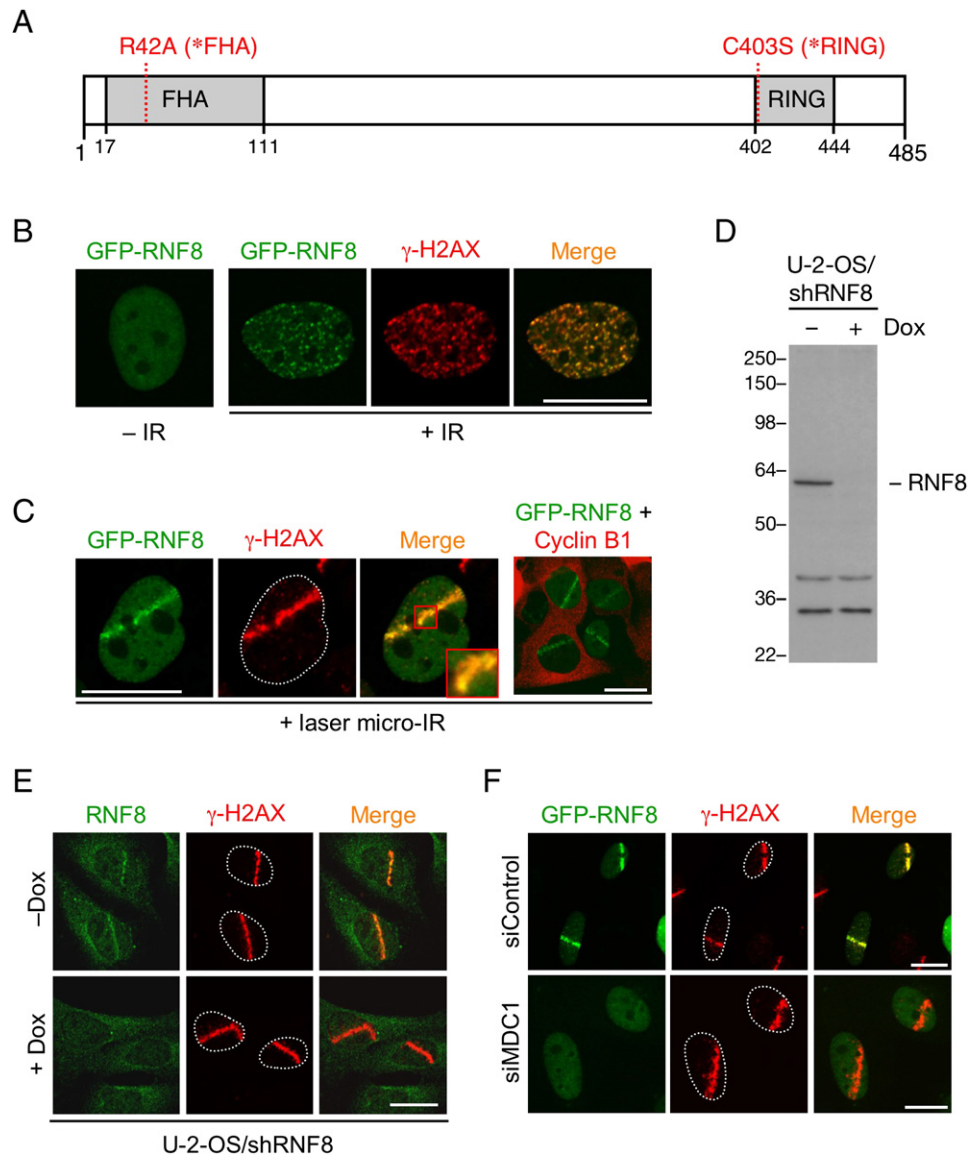


Figure 1. Accumulation of RNF8 at the DSB Sites Is Regulated by MDC1

(A) Schematic structure of human RNF8. Positions of residues mutated to generate RNF8 *FHA (R42A) and RNF8 *RING (C403S) are indicated.

(B) U-2-OS cells stably expressing GFP-RNF8 (U-2-OS/GFP-RNF8) before (left) and 30 min after (right) exposure to IR (4 Gy) were immunostained for γ -H2AX.

(C) U-2-OS/GFP-RNF8 cells were microirradiated and after 30 min immunostained for γ -H2AX (left) or for cyclin B1 (right). RNF8 accumulates at laser tracks regardless of cyclin B1, indicating that its interaction with the DSB sites is cell cycle independent.

(D) U-2-OS cells conditionally expressing shRNA to RNF8 (U-2-OS/shRNF8) cells were induced or not with Doxycycline (Dox) for 48 hr and analyzed by immunoblotting with a rabbit antibody to RNF8.

(E) U-2-OS/shRNF8 cells were induced or not with Dox for 48 hr, exposed to laser microirradiation, and 1 hr later coimmunostained with antibodies to RNF8 and γ -H2AX. WCE, whole-cell extract; scale bar, 10 μ m.

(F) U-2-OS/GFP-RNF8 cells were transfected with the indicated siRNA oligonucleotides for 96 hr, microirradiated as in (C), and immunostained for γ -H2AX. Scale bars, 10 μ m.

Phosphorylation of MDC1 Determines Retention of RNF8 at the DSB Sites

To test the significance of the MDC1-RNF8 interaction directly in cells, we downregulated endogenous MDC1 by shRNA (Bekker-Jensen et al., 2006) and reintroduced

into these cells either WT or the 3A version of MDC1 (both full-length and resistant to the shRNA) together with GFP-RNF8. As expected, the MDC1 knockdown abolished accumulation of GFP-RNF8 at the sites of DNA damage (Figure 2G, top). Strikingly, although MDC1-WT

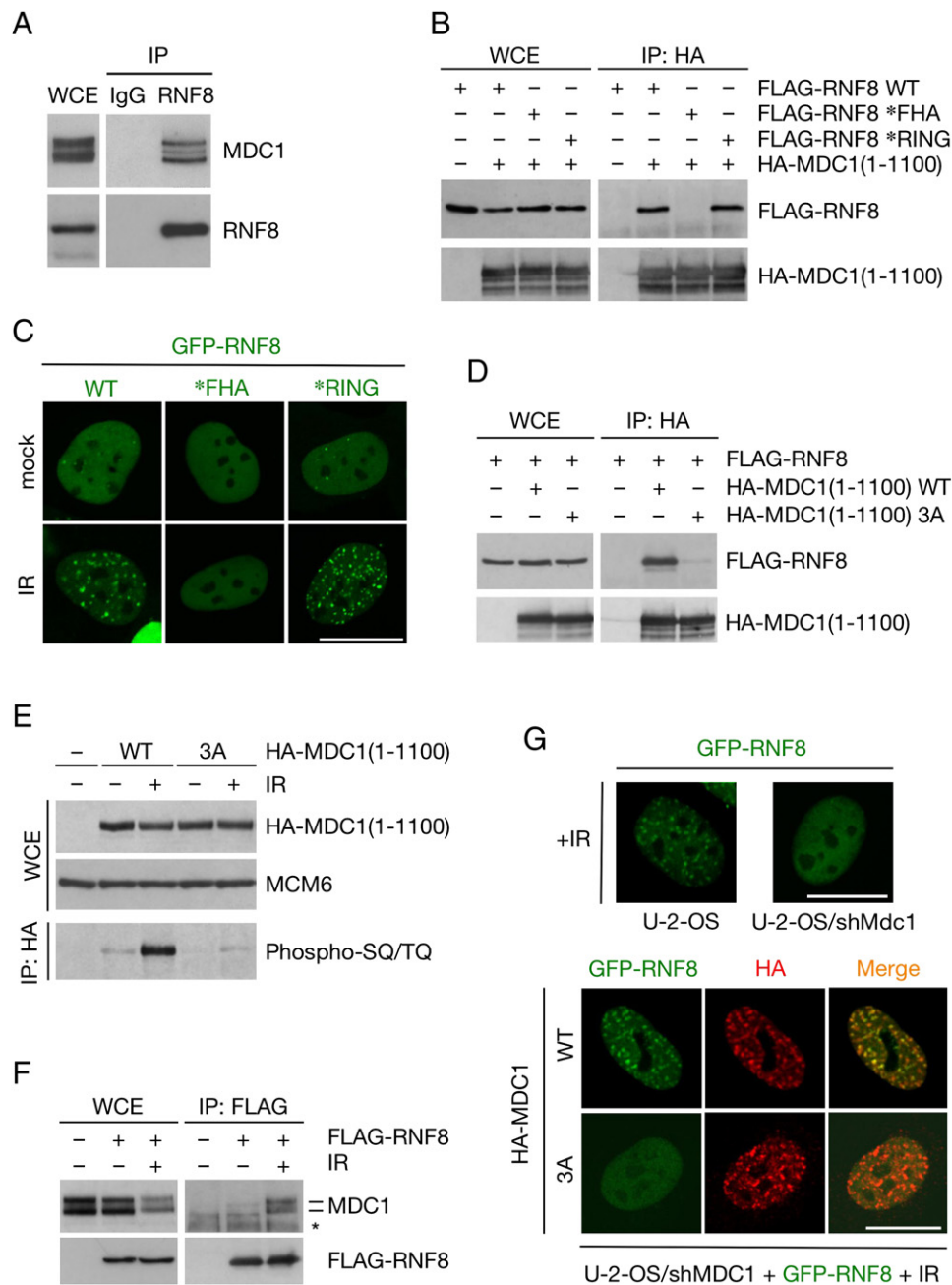


Figure 2. The FHA Domain of RNF8 Interacts with Phosphorylated MDC1

(A) Lysates from HEK293T cells were immunoprecipitated with control or RNF8-specific antibodies followed by immunoblotting with antibody to MDC1.

(B) HEK293T cells were cotransfected with the HA-tagged N-terminal fragment of MDC1 (amino acids 1–1100) and the indicated versions of FLAG-RNF8. Interactions between MDC1 and RNF8 were assessed by immunoprecipitation (IP) of HA-tagged proteins followed by immunoblotting with anti-FLAG antibody.

(C) U-2-OS cells stably expressing wild-type (WT), FHA-deficient (*FHA), or RING-deficient (*RING) forms of GFP-RNF8 were left untreated (top) or exposed to 4 Gy of IR (bottom). Images were acquired after 30 min.

(D) HEK293T cells were cotransfected with indicated combinations of plasmids, and association between RNF8 and MDC1 was analyzed by coimmunoprecipitation as in (A).

(E) HEK293T cells transfected with HA-tagged WT or 3A fragments of MDC1 (1–1100) were exposed or not to IR (10 Gy). One hour later, the extent of MDC1 phosphorylation was assayed by immunoprecipitation with anti-HA antibody followed by immunoblotting with the phospho-SQ/TQ antibody. MCM6 is a loading control. WCE, whole-cell extract.

(F) U-2-OS cells were transfected with FLAG-RNF8 and exposed or not to IR (10 Gy). One hour later, binding between ectopic RNF8 and endogenous

and MDC1-3A were expressed to similar levels (Figure S3A) and formed readily discernible IR-induced foci (Figure 2G, bottom), only the WT protein was able to restore GFP-RNF8 accumulation at the DSB sites (Figure 2G, bottom). Interestingly, while mutation of the T-Q-X-F clusters completely uncoupled MDC1 from RNF8 (Figures 2D and 2G), the same MDC1-3A mutant remained fully proficient to interact with NBS1 (Figure S3B) and support NBS1 focus formation (Figure S3C). Because NBS1 also contains an FHA domain, which is required for its interaction with MDC1 and accumulation at the DSB sites (Lukas et al., 2004a), these data support the emerging concept of MDC1 as a molecular matchmaker capable of organizing multiple signaling and repair factors in the vicinity of DNA breaks and suggest that the main purpose of the ATM-mediated phosphorylation of the T-Q-X-F clusters is to recruit RNF8.

RNF8 Rapidly Assembles at the DSB-Flanking Chromatin

To investigate the function of RNF8 at the sites of DNA damage, we applied a kinetic assay based on micro-laser-generated DSBs coupled with a real-time imaging of protein redistribution (Bekker-Jensen et al., 2006; Lukas et al., 2003). By this approach, we found that the accumulation of GFP-RNF8 in the microirradiated regions was extremely rapid: the first signs of local concentration of GFP-RNF8 were detectable in less than a minute, and the steady-state accumulation in the DSB areas was reached between 6 and 8 min after microirradiation (Figure 3A, top). We noticed that while the assembly kinetics of GFP-RNF8 was similar to that of GFP-MDC1 (Figure 3A, middle), it appeared faster than the accumulation of GFP-BRCA1 (Figures 3A, bottom and S1C). This prompted us to compare the kinetic parameters of all core components of the DSB-flanking chromatin under strictly identical conditions (Bekker-Jensen et al., 2005, 2006; Lukas et al., 2004a). A quantitative analysis of the fluorescence intensities of MDC1, NBS1, 53BP1, BRCA1, and RNF8 (all GFP-tagged, stably expressed in an isogenic parental cell line, and tested for their functionality) revealed that their accumulation at the DSB-flanking chromatin clusters into two distinct kinetic groups: the “early” group comprising MDC1, NBS1, and RNF8, followed by the “late” group including 53BP1 and BRCA1 (Figure 3B). The delayed assembly of BRCA1 was confirmed at the level of endogenous proteins by comparing its accumulation with that of 53BP1, the known late component of the DSB-modified chromatin (Bekker-Jensen et al., 2005) (Figure S4A). Conversely, we found that endogenous RNF8 accumulated at the DSB sites as early as MDC1,

the most upstream protein to arrive at the γ -H2AX-marked chromatin (Figure S4B). Finally, the assembly of ATR, a protein that specifically interacts with single-stranded DNA generated by DSB resection (Cortez et al., 2001; Bekker-Jensen et al., 2006), was significantly delayed compared to both early and late chromatin assembly waves (Figure 3B), suggesting that the chromatin response in general precedes the DNA-end resection. Collectively, these results demonstrated that our experimental conditions were sensitive enough to temporally dissect the DSB-induced chromatin formation, and that RNF8 is among the first proteins to assemble in this compartment.

A Ubiquitin-Regulated Event Couples the Rapid and Delayed Accumulation of Proteins at the DSB-Modified Chromatin

The finding that the accumulation of 53BP1 and BRCA1 at DSBs was delayed, dependent on MDC1 (Bekker-Jensen et al., 2005, 2006; Lou et al., 2003) yet each independent of the other (Figure S5), suggested that both 53BP1 and BRCA1 share a common, MDC1-regulated denominator required for their productive retention in the DSB-flanking chromatin. Since RNF8 binds MDC1, accumulates rapidly at the DSB sites, and contains a RING domain typical for the E3 ubiquitin ligases (Ito et al., 2001; Plans et al., 2006), we reasoned that it, and its enzymatic activity, might couple the assembly of MDC1 with the ensuing accumulation of 53BP1 and BRCA1.

To test this hypothesis, we first asked whether regulatory ubiquitylation as such contributes to the accumulation of DSB regulators on the DNA damage-modified chromatin. We exploited the recent findings showing that inhibition of the 26S proteasome causes a rapid depletion of free nuclear ubiquitin due to accumulation of non-degraded polyubiquitylated proteins in the cytosol (Dantuma et al., 2006). Indeed, also in our cellular system proteasome inhibitors such as MG132 triggered progressive translocation of GFP-ubiquitin, as well as the ubiquitin-protein conjugates, from the nucleus to the cytoplasm, a process that was completed between 60 and 90 min after MG132 addition (Figure S6A). This was accompanied by a loss of monoubiquitylated histones (Figure S6B), confirming a severe impairment of regulatory ubiquitylations in the nucleus (Dantuma et al., 2006). Strikingly, such depletion of free nuclear ubiquitin had a very differential impact on the ability of proteins to accumulate at the DSB-flanking chromatin. When cells were pretreated with MG132 and then subjected to laser microirradiation, the pattern and extent of the γ -H2AX-decorated chromatin developed normally, and MDC1, NBS1, and RNF8 (the early

MDC1 was monitored by immunoprecipitation with anti-FLAG antibody followed by immunoblotting with anti-MDC1 antibody (the lower MDC1 signal in lane 3 is due to increased chromatin retention of MDC1 after DNA damage). Asterisk indicates a crossreacting band.

(G) U-2-OS cells, or their derivatives stably expressing the MDC1-targeting shRNA (U-2-OS/shMDC1), were transiently transfected with GFP-RNF8 and exposed to IR (4 Gy, 30 min). The ability of GFP-RNF8 to form IR-induced foci was monitored by confocal microscopy (top). U-2-OS/shMDC1 cells were cotransfected with GFP-RNF8 and the indicated versions of HA-tagged MDC1 (all in the context of full-length MDC1), exposed to IR (4 Gy, 30 min), and immunostained with anti-HA antibody (bottom). Scale bars, 10 μ m.

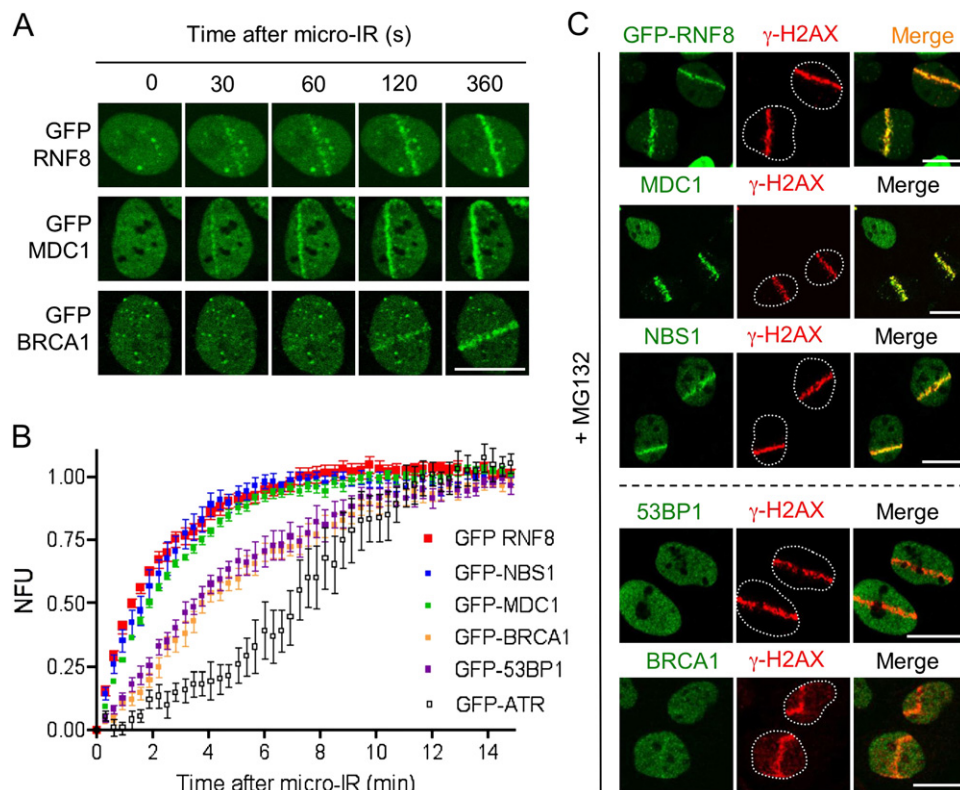


Figure 3. Protein Assembly at the DSB-Flanking Chromatin Follows Two Distinct Temporal Waves

(A) U-2-OS cell lines stably expressing the indicated GFP-tagged proteins were exposed to laser microirradiation followed by a real-time recording of the protein assembly kinetics.

(B) U-2-OS cell lines were assayed as in (A). The fluorescence intensity values in the microirradiated areas were pooled from 10 independent cells per each protein and plotted on a time scale. NFU, normalized fluorescence units. Error bars represent twice the standard error of the normalized data at the respective time points.

(C) U-2-OS/GFP-RNF8 cells (top) or the parental U-2-OS cells (the remaining panels) were incubated for 90 min with MG132, microirradiated by the laser, and after an additional 30 min immunostained with the indicated antibodies. Scale bars, 10 μ m.

kinetic group) accumulated at the DSB sites (Figure 3C, top panels). In contrast, the accumulation of BRCA1 and 53BP1 (the late kinetic group) was abrogated under these conditions (Figure 3C, bottom panels). Consistently, when assayed in cells that had been first microirradiated and only then challenged with MG132, 53BP1 (the late assembly group) but not NBS1 (the early assembly group) dissociated from the microirradiated compartments with the kinetics that mirrored the pace of the nuclear ubiquitin depletion (Figure S6A). Thus, while regulatory ubiquitylation is not required for the initial DSB-induced chromatin response, it appears essential for generating conditions permissive for the second wave of protein accumulation.

RNF8 Ubiquitylates the DSB-Flanking Chromatin and Promotes Accumulation of 53BP1 and BRCA1 in This Compartment

We then designed two independent RNF8-targeting siRNA oligonucleotides, each of which efficiently downregulated RNF8 (Figure S7A). Strikingly, RNF8 knockdown essentially recapitulated chemical depletion of the free

nuclear ubiquitin by allowing normal assembly of MDC1 and NBS1 (Figure 4A, left panels) but preventing accumulation of 53BP1 and BRCA1 at the DSB-flanking chromatin (Figure 4A, right panels). The residual BRCA1 retention in the microirradiated regions was not unexpected given that a fraction of BRCA1 directly binds DNA (Paull et al., 2001), and that this type of interaction is independent of chromatin (Bekker-Jensen et al., 2006). Larger magnification confirmed that the RNF8 knockdown reduced BRCA1 accumulation to small subchromatin “microfoci” typical for ssDNA-binding proteins (Figure 4A, insets). Independent experiments confirmed that downregulation of RNF8 did not prevent DSB resection and formation of the RPA-coated ssDNA compartments (Figure S7B).

Consistent with earlier studies reporting local ubiquitylation in the IR-induced nuclear foci (Morris and Solomon, 2004; Polanowska et al., 2006) we noticed that laser microirradiation induced local accumulation of conjugated ubiquitin (Figure 4B). Remarkably, this was drastically impaired both by depletion of nuclear ubiquitin (achieved by a short treatment with MG132 before microirradiation) and

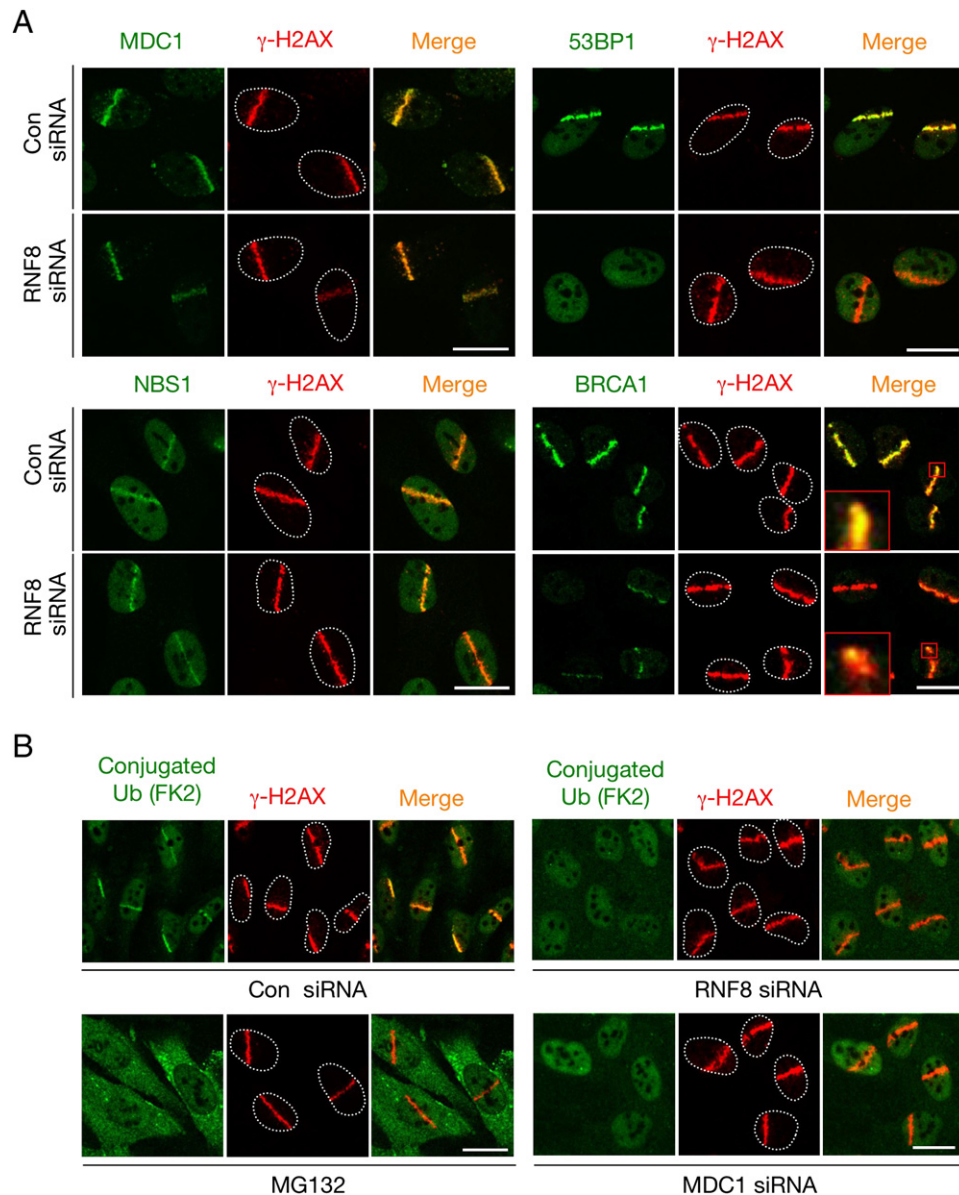


Figure 4. Knockdown of RNF8 Impairs Accumulation of 53BP1, BRCA1, and Conjugated Ubiquitin at the DSB-Flanking Chromatin
 (A) U-2-OS cells were transfected with control or RNF8-targeting siRNA oligonucleotides, microirradiated, and 1 hr later immunostained with the indicated antibodies.

(B) U-2-OS cells were transfected with the indicated siRNA oligonucleotides or treated for 90 min with MG132 as indicated, microirradiated, incubated for 1 hr, and coimmunostained with antibodies to conjugated ubiquitin (FK2) and γ -H2AX. Scale bars, 10 μ m.

by siRNA-mediated knockdown of RNF8 (Figure 4B). Although knockdown of BRCA1 also reduced the DSB-associated accumulation of conjugated ubiquitin as previously reported (Morris and Solomon, 2004; Polanowska et al., 2006), the effect of RNF8 was consistently much more dramatic (Figures 4B, S8A, and S8B) and comparable to that achieved by depletion of MDC1, the mediator of RNF8 recruitment to the DSB-flanking chromatin (Figure 4B). Together, these data suggest that the RNF8 ubiquitin ligase directly contributes to DSB-induced ubiquitylations that in

turn function as an important trigger for 53BP1 and BRCA1 retention in the neighboring chromatin. In support of this conclusion, knockdown of RNF8 abrogated DSB retention of RAP80 (Figure 5A), a ubiquitin-binding protein that is essential for BRCA1 recruitment to the DSB sites (see Introduction). Interestingly, RNF8 remained associated with the DSB sites as long as these were marked by γ -H2AX (Figure S4C), suggesting that its activity facilitates accumulation of BRCA1 and 53BP1 in the vicinity of DNA breaks until these are productively repaired.

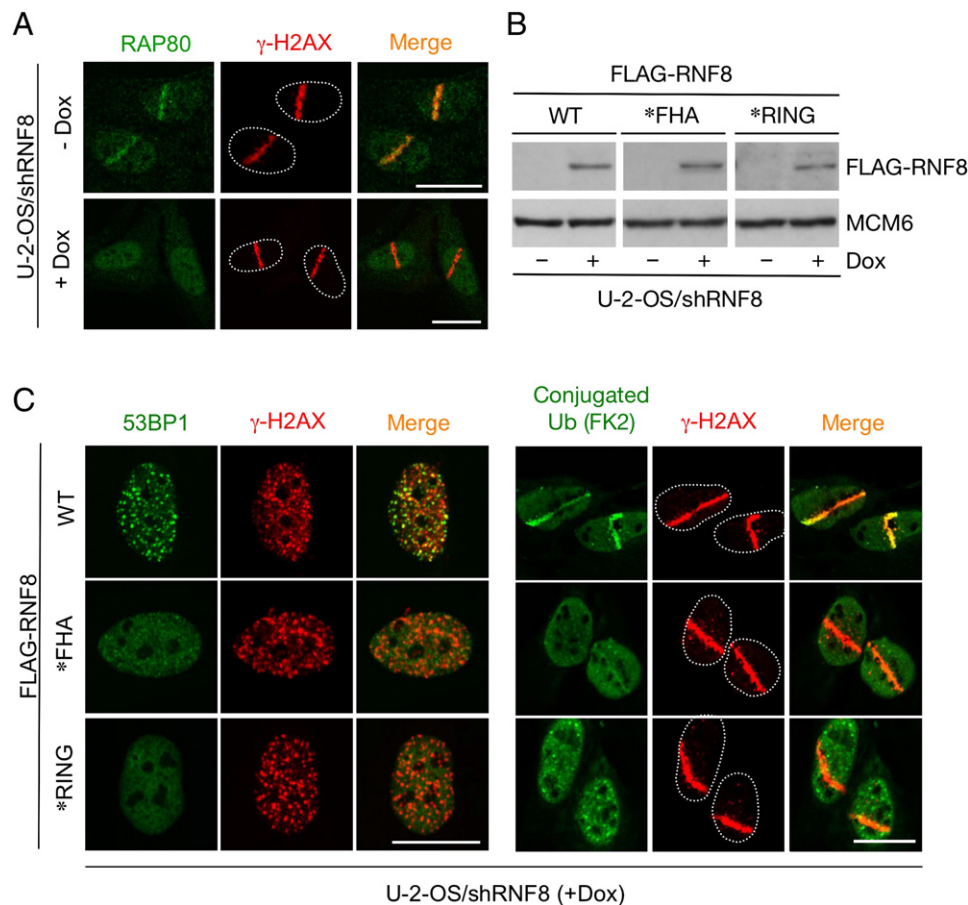


Figure 5. Local Concentration and Catalytic Activity of RNF8 Determine Retention of 53BP1 at the DSB-Flanking Chromatin

(A) U-2-OS/shRNF8 cells were induced or not with Dox for 48 hr, exposed to laser microirradiation, and 1 hr later coimmunostained with antibodies to RAP80 and γ -H2AX.

(B) U-2-OS/shRNF8 cells engineered to induce various alleles of FLAG-tagged, shRNA-resistant RNF8 were incubated or not with Dox, and the expression of the induced RNF8 proteins was monitored by immunoblotting with anti-FLAG antibody.

(C) U-2-OS/shRNF8/FLAG-RNF8 cells from (B) were induced with doxycycline (Dox) for 48 hr and exposed to IR (4 Gy) (left) or microirradiated by the laser (right). After 1 hr, the cells were coimmunostained with antibodies to γ -H2AX and 53BP1 (left) or conjugated ubiquitin (FK2) (right). Scale bars, 10 μ m.

To test the impact of RNF8 on the DSB-induced chromatin maturation in vivo, we generated cell lines allowing a conditional replacement of the endogenous RNF8 by the WT, *FHA, or *RING versions of RNF8 achieved by a doxycycline-dependent induction of the RNF8-targeting shRNA combined with a simultaneous induction of the respective RNF8 alleles resistant to the shRNA (Figure 5B). Significantly, while reintroduction of WT RNF8 restored 53BP1 focus formation in IR-treated cells (Figure 5C, left), and accumulation of conjugated ubiquitin in laser-generated DSB tracks (Figure 5C, right), both the *FHA (active but unable to accumulate at DSBs) and *RING (able to accumulate at DSBs but inactive) mutants failed to do so (Figure 5C). Thus, both MDC1-mediated accumulation of RNF8 and its RING-finger-associated ubiquitin ligase activity are required for local increase of DSB-associated ubiquitylations and the ensuing accumulation of repair proteins in this compartment.

DSB-Associated RNF8 Promotes Ubiquitylation of H2A

To elucidate the identity of the RNF8-mediated ubiquitin conjugates at DSBs, we applied fluorescence recovery after photobleaching (FRAP) (Lukas et al., 2004a; Bekker-Jensen et al., 2005) and analyzed the intranuclear dynamics of the WT and the catalytically-inactive (*RING) versions of RNF8. While the mobility of both proteins in the undamaged nucleoplasm was similar, their dynamics at the microlaser-generated DSBs were markedly different (Figure 6A). The mean residence time at DSBs of the inactive RNF8 extended up to 14.7 ± 0.1 s, which was more than three times longer than the WT protein (4.3 ± 0.1 s). Together with the biochemical analysis showing significant enrichment of the RING-deficient RNF8 in chromatin fractions (Figure S9A), these data suggest that the RNF8 substrate (from which the catalytically inactive

RNF8 may not readily dissociate) could be a constitutive component of chromatin.

To test this hypothesis, we examined whether RNF8 functionally interacts with H2A, a core histone that undergoes increased monoubiquitylation in response to UV-induced DNA damage (Bergink et al., 2006). Indeed, at least five independent pieces of evidence indicated a functional link between RNF8 and H2A. First, RNF8 physically interacted with H2A, and this interaction was much stronger after disrupting the RING domain of RNF8 (Figure 6B). Second, using an optimized assay to monitor histone ubiquitylation (Wang et al., 2006) we could detect an increase in the FLAG-H2A ubiquitylation of cells exposed to IR, and this increase was reduced after knocking down endogenous RNF8 (Figure 6C). Third, consistent with the requirement of MDC1 for RNF8 recruitment, MDC1 knockdown abrogated the IR-induced ubiquitylation of FLAG-H2A (Figure S9B). Fourth, the recombinant RNF8, but not the RING-deficient mutant, catalyzed ubiquitylation of H2A in an *in vitro* ubiquitylation assay (Figure 6D). Finally, an antibody specific to ubiquitylated H2A detected a clear accumulation of ubiquitin species at the microlaser-generated DSB sites, and this H2A-ubiquitin accumulation was inhibited by RNF8 knockdown (Figure 6E). Thus, H2A emerged as a strong candidate substrate of the DSB-associated RNF8 ubiquitin ligase. Interestingly, we noticed that depletion of RNF8 partially decreased also the overall H2A ubiquitylation even in nonirradiated cells (Figure 6C). Although we cannot exclude a damage-unrelated function of RNF8, this observation may also reflect spontaneous DNA breakage associated with replication errors.

To test whether RNF8 targets other histones, we extended the *in vitro* ubiquitylation assay and tested the ability of RNF8 to catalyze ubiquitylation of H2A, H2AX, H2B, and H3. While H2A and its structurally related variant H2AX were robustly ubiquitylated under these conditions, H2B and H3 were modified much less efficiently (Figure S9C). Interestingly, the ubiquitylation pattern of H2AX resembled that of H2A, and in both cases, WT RNF8 (but not the RING-deficient mutant) catalyzed attachment of multiple ubiquitin moieties (Figures 6D and S9C). Consistently, the oligo-ubiquitylation of FLAG-tagged H2A (Figure 6C) and to a lesser extent H2AX (Figure S9D) was also observed in cells, and the main ubiquitin species were induced by IR in an RNF8-dependent manner. Finally, similar oligo-ubiquitylated (and IR-inducible) H2A species were also observed on endogenous H2A immunopurified from native cell extracts by an antibody to ubiquitylated H2A (Figure S9E). Together, these data suggest that RNF8 increases local ubiquitylation of H2A (and to some extent also H2AX), and that these histone modifications closely correlate with the transition of the DSB-flanking chromatin to a state permissive for BRCA1 and 53BP1 accumulation.

RNF8 Facilitates Survival after a DSB-Generating Insult

Finally, we tested the impact of RNF8 on DNA-damage signaling and cell survival in an isogenic cell line capable

of conditional RNF8 knockdown. Reduction of RNF8 levels had little effect on cell-cycle progression in undamaged cells, indicating that the effect of RNF8 on BRCA1 and 53BP1 was not simply a consequence of a cell-cycle arrest (Figure S7C). In addition, the IR-induced phosphorylation of four independent ATM/ATR targets (SMC1, p53, CHK2, and CHK1) appeared normal (Figure S7D). This is consistent with our previous findings (Figures 3C and 4A) that RNF8, and the dynamic nuclear ubiquitylations, neither affect accumulation of MDC1 and NBS1 at the DSB sites (both events are known to facilitate ATM signaling [Falck et al., 2005; Lou et al., 2006; You et al., 2005]) nor interfere with the DSB resection and formation of the ssDNA compartments (Figure S7B), the structures required for activation of the ATR-Chk1 pathway (Cortez et al., 2001; Jazayeri et al., 2006). In agreement with these results, we did not observe significant defects in the cell-cycle checkpoints after RNF8 knockdown (our unpublished observations). We then tested whether the same degree of RNF8 downregulation would have any effect on clonogenic survival after a DSB-generating insult. When challenged with moderate doses of IR (2 Gy) the transient knockdown of RNF8 significantly reduced the fraction of surviving cells (Figure 6F). Together with the lack of obvious defects in ATM/ATR-mediated phosphorylations (Figure S7D) and the strong impairment of 53BP1 and BRCA1 focus formation in the absence of RNF8 (Figure 4A), these data suggest that the increased radiation sensitivity of RNF8-deficient cells reflects the inability to retain BRCA1 and 53BP1 (and possibly other genome surveillance factors) in the vicinity of the chromosomal lesions.

DISCUSSION

Our results suggest that RNF8 functions at the crossroads between two main stages of the DSB-induced chromatin response (Figure 7). While the first stage is competent to support DSB signaling, it is not permissive to increase local concentration of repair factors such as 53BP1 and BRCA1. This is only achieved in the second step, and the transition into this “mature” stage is critically dependent on the RNF8 ubiquitin ligase. The key question posed by this model is how does RNF8 promote local accumulation of proteins as diverse as 53BP1 and BRCA1? Two major scenarios come to mind. The first (“direct”) scenario assumes that the RNF8-mediated histone ubiquitylation recruits the molecular machinery that tethers both proteins to the DSB-modified chromatin. According to the second (“indirect”) scenario, RNF8 promotes a higher-order chromatin restructuring to facilitate local exposure of constitutive chromatin marks that in turn increase local affinity for 53BP1 and BRCA1. Below we discuss the fact that both models are plausible and not necessarily mutually exclusive.

The direct scenario is supported by the four recent studies showing that the ubiquitin-binding protein RAP80 is required to target BRCA1 to DSBs (Kim et al., 2007;

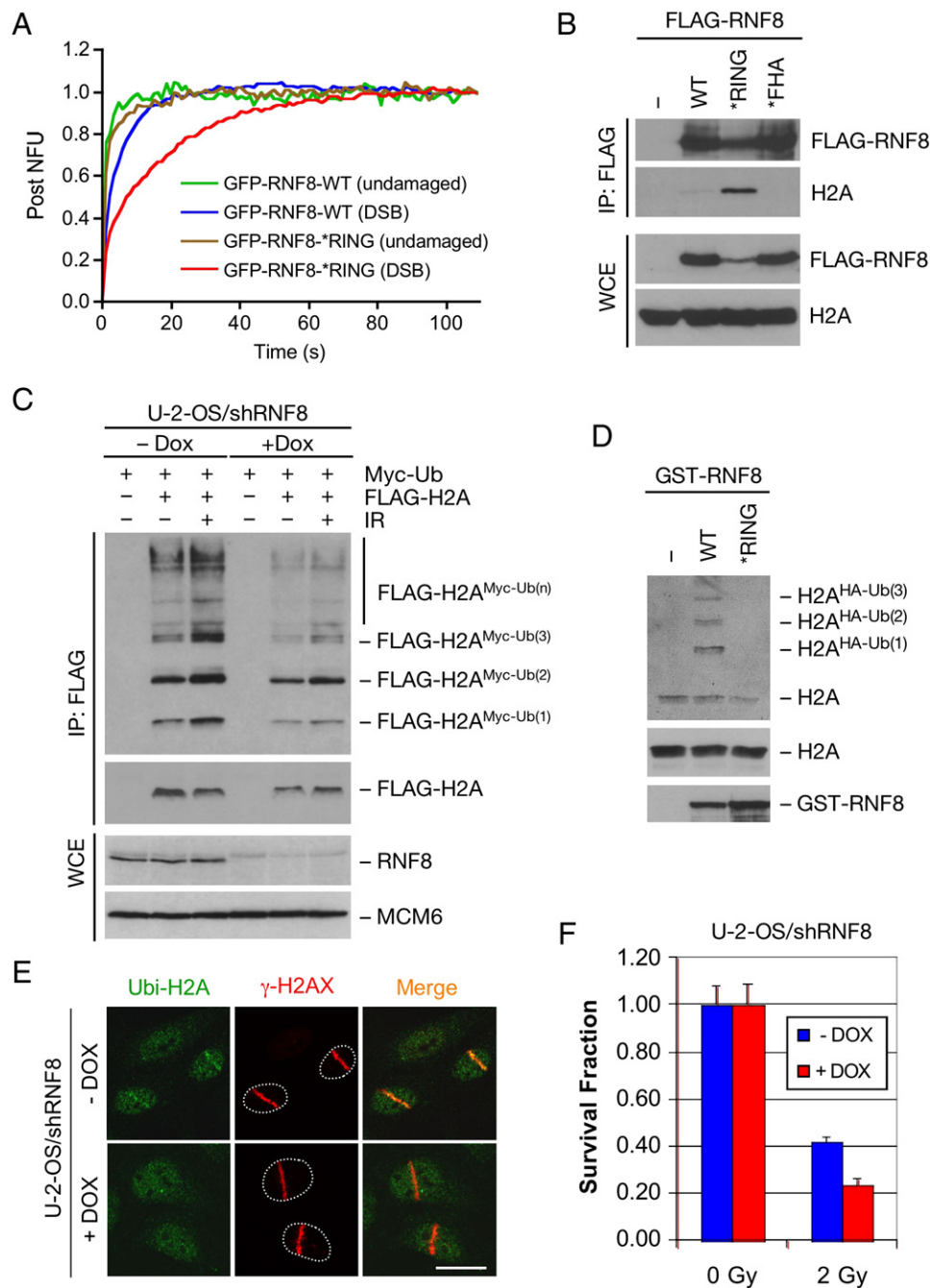


Figure 6. DSBs Trigger RNF8-Dependent Ubiquitylation of H2A

(A) U-2-OS cell lines stably expressing the indicated GFP-tagged RNF8 constructs were exposed to laser microirradiation. After 1 hr, the GFP-associated fluorescence was bleached in small rectangular regions ($2 \times 2 \mu\text{m}$) placed either to the undamaged nucleoplasm or over the laser-generated DSB tracks, and the fluorescence recovery in these regions was determined by repetitive image acquisition. The recovery curves were derived from 10 independent cells for each condition.

(B) HEK293T cells were transfected with indicated FLAG-RNF8 constructs. Cells were lysed in EBC buffer containing 500 mM NaCl, and extracts were subjected to immunoprecipitation with anti-FLAG agarose beads. Bound complexes were analyzed by immunoblotting with the indicated antibodies.

(C) U-2-OS/shRNF8 cells were left untreated or induced by addition of Dox. Twenty-four hours later, cells were transfected with indicated constructs for an additional 24 hr and mock-treated or exposed to IR (20 Gy) for 1 hr. Total cell extracts were prepared by lysing cells in denaturing buffer and subjected to immunoprecipitation with anti-FLAG agarose beads under denaturing conditions. Bound complexes were analyzed by immunoblotting.

(D) The capability of purified GST-RNF8 proteins to ubiquitylate Histone H2A in vitro was analyzed as described in Experimental Procedures. Reaction mixtures were resolved by SDS-PAGE and analyzed by immunoblotting.

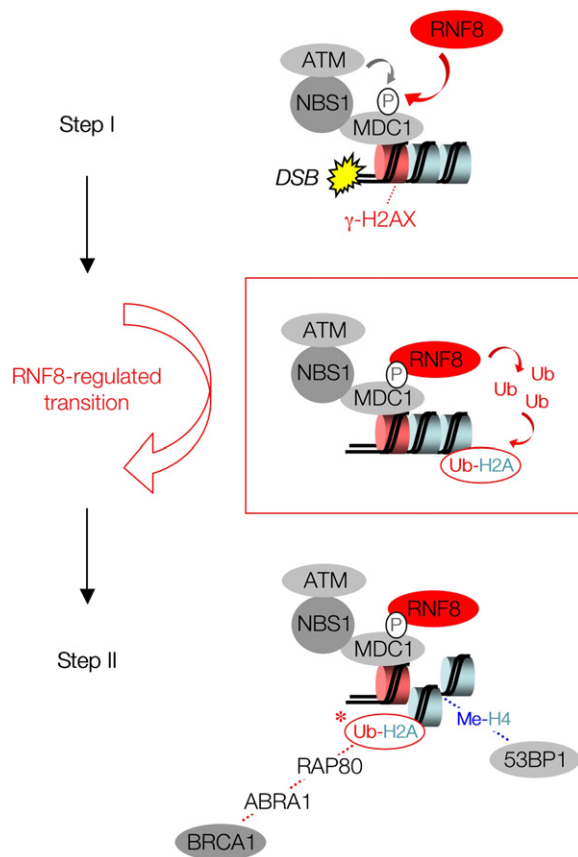


Figure 7. A Schematic Model of the Two-Step Chromatin Response to DSBs and the Involvement of RNF8 in This Process RNF8 recruitment to the DSB sites is triggered by the ATM-mediated phosphorylation of MDC1 (Step I). Once recruited, RNF8 catalyzes ubiquitylation of H2A. At this point, the DSB-flanking chromatin becomes competent to recruit and accumulate 53BP1 and BRCA1 (Step II). Asterisk indicates that H2AX, a structural variant of H2A, can also be targeted by RNF8 and may contribute to the transition between the initial and advanced stages of the DSB-induced chromatin response. See Discussion for details.

Sobhian et al., 2007; Wang et al., 2007; Yan et al., 2007). Although identification of the ubiquitin-dependent step in BRCA1 focus formation was important, none of these studies identified the enzymatic machinery that would locally ubiquitylate the DSB compartments and allow their recognition by RAP80. Our study may provide this missing link and allow us to describe the BRCA1 retention at the DSB-modified chromatin in a more complete fashion (Figure 7). Thus, the BRCA1 “assembly line” starts with phosphorylation of H2AX, followed by formation of the γ -H2AX-MDC1 complex, increased local concentration of ATM, phosphorylation of MDC1, and its recognition

by the FHA domain of RNF8. The resulting recruitment of RNF8 increases local ubiquitylation of histones such as H2A and H2AX, which may provide a direct recognition signal for the ubiquitin-interaction domains of RAP80. The entire pathway is then completed by ABRA1, a mediator protein that can simultaneously bind to RAP80 and the BRCT domains of BRCA1 (Wang et al., 2007).

In contrast to BRCA1, the mechanism of the DSB-induced accumulation of 53BP1 is less clear. While our results clearly implicate a ubiquitin-dependent step in this process, the link between the RNF8-mediated H2A/H2AX ubiquitylation and the Tudor-dependent binding of 53BP1 to methylated H3 or H4 remains elusive. One possibility is that RNF8, and the DSB-associated histone ubiquitylations, may also have an indirect impact on maturation of the DSB-flanking chromatin (Figure 7). In support for this indirect scenario, we noticed that genetic ablation of the TRRAP-TIP60 histone acetyltransferase (HAT) generated a phenotype that was remarkably similar to what we have observed after RNF8 knockdown (Murr et al., 2006; this study). In each case, assembly of MDC1 at the DSB sites was normal but accumulation of both 53BP1 and BRCA1 was impaired. Because histone hyperacetylation is often coupled to the less compacted chromatin (Kouzarides, 2007), it is possible that local relaxation of the DSB-flanking regions contributes to the full-scale retention of BRCA1 and 53BP1 in this compartment, and that both histone ubiquitylation and acetylation contribute to this process. Our findings that RNF8 accumulates at DSBs extremely rapidly suggest that RNF8 may operate upstream of the TRRAP-TIP60 complex, possibly by stimulating its access to the DSB-flanking chromatin and/or by enhancing its HAT activity. Such an indirect scenario is attractive not only because it suggests a way to unmask cryptic methyl residues required for 53BP1 recruitment but also because it provides an opportunity to amplify the RAP80-mediated signal to locally concentrate BRCA1. It is important to realize that H2A and H2AX are also ubiquitylated in unstressed cells. However, it is also possible that in the context of intact interphase chromatin, the bulk of these ubiquitin conjugates may not be readily accessible to interact with ubiquitin-binding factors. We can imagine that even a modest increase of RNF8-mediated histone ubiquitylation (perhaps in conjunction with locally enhanced HAT activity) may alter chromatin configuration to an extent that would also expose the pre-existing histone-associated ubiquityl groups and thereby nucleate a more efficient “affinity trap” for RAP80 and indeed the entire machinery that concentrates BRCA1 in the vicinity of unrepaired DNA breaks.

A recent study reported H2A ubiquitylation after ultraviolet (UV)-induced DNA damage (Bergink et al., 2006).

(E) U-2-OS/shRNF8 cells were induced or not with Dox for 48 hr, exposed to laser microirradiation, and 1 hr later coimmunostained with antibodies to ubiquitylated H2A and γ -H2AX.

(F) U-2-OS/shRNF8 cells were induced or not with Dox for 24 hr, split by a limited dilution (+ Dox), and after an additional 24 hr exposed to the indicated doses of IR. Subsequently, the cells were incubated for an additional 14 days and stained with crystal violet. Colonies containing more than 50 cells were counted. The experiment was carried out in triplicates. Error bars represent standard error; scale bars, 10 μ m.

Although the UV-induced H2A ubiquitylation required ATR (conceptually similar to the ATM-dependent RNF8 regulation described here), some aspects of its regulation differed from the DSB response. Thus, the UV-induced H2A ubiquitylation was mediated by RNF2 (also known as RING1B), a canonical ubiquitin ligase required for H2A ubiquitylation associated with transcriptional silencing (de Napoles et al., 2004; Wang et al., 2004). In addition, it occurred relatively late after UV exposure and did not require H2AX (Bergink et al., 2006). Despite these differences (likely reflecting the fundamentally distinct repair machineries involved in DSBs and UV lesions), H2A ubiquitylation emerges as a general histone modification induced by DNA damage. While the rapid H2A ubiquitylation after DSBs serves to retain proteins engaged with various aspects of DSB repair, the delayed H2A ubiquitylation after UV may facilitate events that have high demands on a permissive chromatin configuration and are specific for UV-generated lesions such as repair of actively transcribed DNA strands.

Our findings, and the accompanying paper by Chen and colleagues, who reached similar conclusions (Huen et al., 2007 [this issue of *Cell*]), complement the emerging role of regulatory ubiquitylations in diverse aspects of the DNA-damage response by identifying an RNF8-dependent step during the maturation of the DSB-induced chromatin. We propose that the key purpose of the RNF8-controlled transition to the advanced stages of the DSB-induced chromatin response is to concentrate repair factors in the vicinity of DNA breaks to the threshold required for timely and accurate restoration of genome integrity. Both BRCA1 and 53BP1 are established tumor suppressors (Boulton, 2006; Morales et al., 2006; Ward et al., 2005). Identification of RNF8 as an upstream regulator of BRCA1 opens up the possibility that RNF8 might be targeted by mutations in a subset of breast and ovarian cancers, where the sequence of BRCA1 remains unaffected.

EXPERIMENTAL PROCEDURES

Plasmids and RNA Interference

A cDNA for human RNF8 (a gift from Yukio Okano) was inserted by PCR into pEGFP-C1 (Clontech) and pFLAG-CMV2 (Sigma), respectively. The *FHA (R42A) and *RING (C403S) mutations were generated using the QuikChange Site-Directed Mutagenesis Kit (Stratagene). An expression plasmid for HA-MDC1 (1–1100) was generated by insertion of a corresponding MDC1 PCR fragment into pcDNA4/TO (Invitrogen), containing two N-terminal HA-tags. The FLAG-H2A plasmid was a gift from Moshe Oren. Plasmid transfections were performed using FuGene 6 (Roche). siRNA oligonucleotides (Dharmacon) were synthesized to the following sequences (sense strand): RNF8-1 (5'-GGACAA UUAUGGACAACAA-3'), RNF8-2 (5'-UGCGGAGUAUGAAUUGAA-3'), MDC1 (Goldberg et al., 2003), and GL2 (control) (Mailand et al., 2006). All siRNA transfections were performed with 100 nM siRNA duplexes using Lipofectamine RNAiMAX (Invitrogen). A vector for inducible expression of RNF8-specific shRNA was generated by insertion of 5'-phosphorylated oligos containing the RNF8 target sequence (5'-AC ATGAAGCCGTTATGAAT-3') into pSUPERIOR.puro (Oligoengine). To generate shRNA-insensitive FLAG-RNF8 constructs, the underlined silent mutations (ACATGA~~G~~CG~~G~~TTATGAAT) were introduced into the shRNF8 target sequence in the RNF8 coding region.

Cell Culture

Human U-2-OS osteosarcoma cells and 293T human embryonic kidney cells were grown in DMEM containing 10% fetal bovine serum (GIBCO). Where indicated, the culture medium was supplied by the proteasome inhibitor MG132 (Calbiochem; 5 μ M). U-2-OS cell lines stably expressing GFP-RNF8, FLAG-RNF8, or shRNF8 constructs in a Dox-inducible fashion were generated as described (Mailand et al., 2006). The U-2-OS cell lines stably expressing MDC1-shRNA, GFP-MDC1, GFP-53BP1, GFP-ATR, and NBS1-RFP were described (Bekker-Jensen et al., 2006; Jazayeri et al., 2006). U-2-OS cells stably expressing GFP-BRCA1 together with its heterodimerizing partner FLAG-BARD1 were generated using standard procedures (Bekker-Jensen et al., 2005; Lukas et al., 2004a) and are characterized in Figure S1. IR was delivered by the X-Ray generator (Pantak HF160, 150 kV, 15 mA, dose rate 2.18 Gy/min). Clonogenic survival assay is specified in the figure legends (Figure 7F).

Immunochemical Methods

Immunochemical assays were described (Bekker-Jensen et al., 2005, 2006; Lukas et al., 2004a; Mailand et al., 2006). Rabbit antiserum to RNF8 was raised against a peptide spanning residues 203–217 of human RNF8. Other antibodies included mouse and rabbit antibodies to HA-tag (sc-7392 and sc-805), rabbit polyclonal antibodies to GFP (sc-8334, Santa Cruz), histone H2A (Ab-18255, Abcam), RAP80 (BL2839, Bethyl Laboratories), phospho-SQ/TQ (2851, Cell Signaling), and mouse monoclonal antibodies to conjugated ubiquitin (FK2; Biomol, PW 8810) and to ubiquitylated H2A (05-678, Upstate). The specificity of the latter antibody for ubiquitylated H2A was demonstrated earlier (Baarends et al., 2005). Antibodies to FLAG, MCM6, γ -H2AX, Cyclin B1, MDC1, NBS1, 53BP1, and BRCA1 were described (Bekker-Jensen et al., 2006; Mailand et al., 2006).

Microscopy and Laser Microirradiation

Confocal images were acquired on LSM-510 (Carl Zeiss Microimaging Inc.) mounted on Zeiss-Axiovert 100M equipped with Plan-Neofluar 40 \times /1.3 oil immersion objective. Laser microirradiation to generate local DSBs and conditions for timelapse microscopy were described (Bekker-Jensen et al., 2005, 2006; Lukas et al., 2003, 2004a). FRAP assays including the mathematical analysis of the data were described previously (Lukas et al., 2004a).

Histone Ubiquitylation Assays

Histone ubiquitylation assays were performed essentially as described (Wang et al., 2006). Cells were cotransfected with FLAG-tagged histones and Myc-tagged ubiquitin and dissolved by sonication in denaturing buffer (20 mM Tris, pH 7.5; 50 mM NaCl, 0.5% NP-40; 0.5% Deoxycholate; 0.5% SDS; 1 mM EDTA) containing protease inhibitors. Cell extracts were subjected to immunoprecipitation with anti-FLAG M2 agarose beads (Sigma) under denaturing conditions and purified. Bound material was analyzed by immunoblotting. For *in vitro* ubiquitylation assays, 1 μ g of histones H2A, H2B, H3 (New England Biolabs), or H2AX (Upstate) was incubated in 30 μ l reaction mixture containing 50 mM Tris, pH 7.5; 5 mM MgCl₂; 2 mM NaF; 2 mM ATP; 10 μ M Okadaic acid; 1 mM DTT; 0.1 μ g E1; 0.2 μ g UbchH5c; and 1 μ g HA-ubiquitin (all from Boston Biochem). Two hundred nanograms of bacterially purified, full-length GST-RNF8 was added, and reactions were incubated for 1 hr at 37°C, stopped by the addition of Laemmli Sample Buffer, and resolved by SDS-PAGE. Ubiquitylated histones were detected by immunoblotting as specified in the figure legends.

Supplemental Data

Supplemental Data include nine figures and can be found with this article online at <http://www.cell.com/cgi/content/full/131/5/1131-1141>.

ACKNOWLEDGMENTS

We thank Richard Baer, Junjie Chen, Thanos Halazonetis, Yukio Okano, and Moshe Oren for reagents and Junjie Chen for communicating unpublished results. This work was supported by the Danish Cancer Society, Danish National Research Foundation, European Union (integrated project "DNA Repair" and "Mutant p53"), European Science Foundation (EuroDYNA), Danish Research Council, SSMF Stockholm, and John and Birthe Meyer Foundation.

Received: March 12, 2007

Revised: June 11, 2007

Accepted: September 25, 2007

Published online: November 15, 2007

REFERENCES

- Baarends, W.M., Wassenaar, E., van der Laan, R., Hoogerbrugge, J., Sleddens-Linkels, E., Hoeijmakers, J.H., de Boer, P., and Grootegoed, J.A. (2005). Silencing of unpaired chromatin and histone H2A ubiquitination in mammalian meiosis. *Mol. Cell Biol.* 25, 1041–1053.
- Bekker-Jensen, S., Lukas, C., Melander, F., Bartek, J., and Lukas, J. (2005). Dynamic assembly and sustained retention of 53BP1 at the sites of DNA damage are controlled by Mdc1/NFBD1. *J. Cell Biol.* 170, 201–211.
- Bekker-Jensen, S., Lukas, C., Kitagawa, R., Melander, F., Kastan, M.B., Bartek, J., and Lukas, J. (2006). Spatial organization of the Mamm. Genome surveillance machinery in response to DNA strand breaks. *J. Cell Biol.* 173, 195–206.
- Bergink, S., Salomons, F.A., Hoogstraten, D., Grootuis, T.A., de Waard, H., Wu, J., Yuan, L., Citterio, E., Houtsmuller, A.B., Neeffjes, J., et al. (2006). DNA damage triggers nucleotide excision repair-dependent monoubiquitylation of histone H2A. *Genes Dev.* 20, 1343–1352.
- Botuyan, M.V., Lee, J., Ward, I.M., Kim, J.E., Thompson, J.R., Chen, J., and Mer, G. (2006). Structural basis for the methylation state-specific recognition of histone H4-K20 by 53BP1 and Crb2 in DNA repair. *Cell* 127, 1361–1373.
- Boulton, S.J. (2006). Cellular functions of the BRCA tumour-suppressor proteins. *Biochem. Soc. Trans.* 34, 633–645.
- Cortez, D., Guntuku, S., Qin, J., and Elledge, S.J. (2001). ATR and ATRIP: partners in checkpoint signaling. *Science* 294, 1713–1716.
- Dantuma, N.P., Grootuis, T.A., Salomons, F.A., and Neeffjes, J. (2006). A dynamic ubiquitin equilibrium couples proteasomal activity to chromatin remodeling. *J. Cell Biol.* 173, 19–26.
- de Napoles, M., Mermoud, J.E., Wakao, R., Tang, Y.A., Endoh, M., Apanah, R., Nesterova, T.B., Silva, J., Otte, A.P., Vidal, M., et al. (2004). Polycomb group proteins Ring1A/B link ubiquitylation of histone H2A to heritable gene silencing and X inactivation. *Dev. Cell* 7, 663–676.
- Falck, J., Coates, J., and Jackson, S.P. (2005). Conserved modes of recruitment of ATM, ATR and DNA-PKcs to sites of DNA damage. *Nature* 434, 605–611.
- Fernandez-Capetillo, O., Lee, A., Nussenzweig, M., and Nussenzweig, A. (2004). H2AX: the histone guardian of the genome. *DNA Repair (Amst.)* 3, 959–967.
- Goldberg, M., Stucki, M., Falck, J., D'Amours, D., Rahman, D., Pappin, D., Bartek, J., and Jackson, S.P. (2003). MDC1 is required for the intra-S-phase DNA damage checkpoint. *Nature* 421, 952–956.
- Huen, M.S.Y., Grant, R., Manke, I., Minn, K., Yu, X., Yaffe, M.B., and Chen, J. (2007). RNF8 transduces the DNA-damage signal via histone ubiquitylation and checkpoint protein assembly. *Cell* 131, this issue, ■■■–■■■.
- Huyen, Y., Zgheib, O., Ditullio, R.A., Jr., Gorgoulis, V.G., Zacharatos, P., Petty, T.J., Shestov, E.A., Mellert, H.S., Stavridi, E.S., and Halazonetis, T.D. (2004). Methylated lysine 79 of histone H3 targets 53BP1 to DNA double-strand breaks. *Nature* 432, 406–411.
- Ito, K., Adachi, S., Iwakami, R., Yasuda, H., Muto, Y., Seki, N., and Okano, Y. (2001). N-terminally extended human ubiquitin-conjugating enzymes (E2s) mediate the ubiquitination of RING-finger proteins, ARA54 and RNF8. *Eur. J. Biochem.* 268, 2725–2732.
- Jazayeri, A., Falck, J., Lukas, C., Bartek, J., Smith, G.C., Lukas, J., and Jackson, S.P. (2006). ATM- and cell cycle-dependent regulation of ATR in response to DNA double-strand breaks. *Nat. Cell Biol.* 8, 37–45.
- Kim, H., Chen, J., and Yu, X. (2007). Ubiquitin-binding protein RAP80 mediates BRCA1-dependent DNA damage response. *Science* 316, 1202–1205.
- Kouzarides, T. (2007). Chromatin modifications and their function. *Cell* 128, 693–705.
- Kruhlak, M.J., Celeste, A., Dellaire, G., Fernandez-Capetillo, O., Muller, W.G., McNally, J.G., Bazett-Jones, D.P., and Nussenzweig, A. (2006). Changes in chromatin structure and mobility in living cells at sites of DNA double-strand breaks. *J. Cell Biol.* 172, 823–834.
- Lou, Z., Chini, C.C., Minter-Dykhouse, K., and Chen, J. (2003). Mediator of DNA damage checkpoint protein 1 regulates BRCA1 localization and phosphorylation in DNA damage checkpoint control. *J. Biol. Chem.* 278, 13599–13602.
- Lou, Z., Minter-Dykhouse, K., Franco, S., Gostissa, M., Rivera, M.A., Celeste, A., Manis, J.P., van Deursen, J., Nussenzweig, A., Paull, T.T., et al. (2006). MDC1 maintains genomic stability by participating in the amplification of ATM-dependent DNA damage signals. *Mol. Cell* 21, 187–200.
- Lukas, C., Falck, J., Bartkova, J., Bartek, J., and Lukas, J. (2003). Distinct spatiotemporal dynamics of mammalian checkpoint regulators induced by DNA damage. *Nat. Cell Biol.* 5, 255–260.
- Lukas, C., Melander, F., Stucki, M., Falck, J., Bekker-Jensen, S., Goldberg, M., Lerenthal, Y., Jackson, S.P., Bartek, J., and Lukas, J. (2004a). Mdc1 couples DNA double-strand break recognition by Nbs1 with its H2AX-dependent chromatin retention. *EMBO J.* 23, 2674–2683.
- Lukas, J., Lukas, C., and Bartek, J. (2004b). Mammalian cell cycle checkpoints: signalling pathways and their organization in space and time. *DNA Repair (Amst.)* 3, 997–1007.
- Mailand, N., Bekker-Jensen, S., Bartek, J., and Lukas, J. (2006). Destruction of Claspin by SCFbetaTrCP restrains Chk1 activation and facilitates recovery from genotoxic stress. *Mol. Cell* 23, 307–318.
- Morales, J.C., Franco, S., Murphy, M.M., Bassing, C.H., Mills, K.D., Adams, M.M., Walsh, N.C., Manis, J.P., Rassidakis, G.Z., Alt, F.W., et al. (2006). 53BP1 and p53 synergize to suppress genomic instability and lymphomagenesis. *Proc. Natl. Acad. Sci. USA* 103, 3310–3315.
- Morris, J.R., and Solomon, E. (2004). BRCA1: BARD1 induces the formation of conjugated ubiquitin structures, dependent on K6 of ubiquitin, in cells during DNA replication and repair. *Hum. Mol. Genet.* 13, 807–817.
- Murr, R., Loizou, J.I., Yang, Y.G., Cuenin, C., Li, H., Wang, Z.Q., and Herceg, Z. (2006). Histone acetylation by Trapp-Tip60 modulates loading of repair proteins and repair of DNA double-strand breaks. *Nat. Cell Biol.* 8, 91–99.
- Paull, T.T., Cortez, D., Bowers, B., Elledge, S.J., and Gellert, M. (2001). Direct DNA binding by Brca1. *Proc. Natl. Acad. Sci. USA* 98, 6086–6091.
- Plans, V., Scheper, J., Soler, M., Loukili, N., Okano, Y., and Thomson, T.M. (2006). The RING finger protein RNF8 recruits UBC13 for lysine 63-based self polyubiquitylation. *J. Cell. Biochem.* 97, 572–582.
- Polanowska, J., Martin, J.S., Garcia-Muse, T., Petalcorin, M.I., and Boulton, S.J. (2006). A conserved pathway to activate BRCA1-dependent ubiquitylation at DNA damage sites. *EMBO J.* 25, 2178–2188.

- Shiloh, Y. (2003). ATM and related protein kinases: safeguarding genome integrity. *Nat. Rev. Cancer* 3, 155–168.
- Sobhian, B., Shao, G., Lilli, D.R., Culhane, A.C., Moreau, L.A., Xia, B., Livingston, D.M., and Greenberg, R.A. (2007). RAP80 targets BRCA1 to specific ubiquitin structures at DNA damage sites. *Science* 316, 1198–1202.
- Stewart, G.S., Wang, B., Bignell, C.R., Taylor, A.M., and Elledge, S.J. (2003). MDC1 is a mediator of the mammalian DNA damage checkpoint. *Nature* 421, 961–966.
- Stracker, T.H., Theunissen, J.W., Morales, M., and Petrini, J.H. (2004). The Mre11 complex and the metabolism of chromosome breaks: the importance of communicating and holding things together. *DNA Repair (Amst.)* 3, 845–854.
- Stucki, M., and Jackson, S.P. (2006). gammaH2AX and MDC1: anchoring the DNA-damage-response machinery to broken chromosomes. *DNA Repair (Amst.)* 5, 534–543.
- Stucki, M., Clapperton, J.A., Mohammad, D., Yaffe, M.B., Smerdon, S.J., and Jackson, S.P. (2005). MDC1 directly binds phosphorylated histone H2AX to regulate cellular responses to DNA double-strand breaks. *Cell* 123, 1213–1226.
- Wang, B., Matsuoka, S., Ballif, B.A., Zhang, D., Smogorzewska, A., Gygi, S.P., and Elledge, S.J. (2007). Abraxas and RAP80 form a BRCA1 protein complex required for the DNA damage response. *Science* 316, 1194–1198.
- Wang, H., Wang, L., Erdjument-Bromage, H., Vidal, M., Tempst, P., Jones, R.S., and Zhang, Y. (2004). Role of histone H2A ubiquitination in Polycomb silencing. *Nature* 431, 873–878.
- Wang, H., Zhai, L., Xu, J., Joo, H.Y., Jackson, S., Erdjument-Bromage, H., Tempst, P., Xiong, Y., and Zhang, Y. (2006). Histone H3 and H4 ubiquitylation by the CUL4-DDB-ROC1 ubiquitin ligase facilitates cellular response to DNA damage. *Mol. Cell* 22, 383–394.
- Ward, I.M., Difilippantonio, S., Minn, K., Mueller, M.D., Molina, J.R., Yu, X., Frisk, C.S., Ried, T., Nussenzweig, A., and Chen, J. (2005). 53BP1 cooperates with p53 and functions as a haploinsufficient tumor suppressor in mice. *Mol. Cell. Biol.* 25, 10079–10086.
- Yan, J., Kim, Y.S., Yang, X.P., Li, L.P., Liao, G., Xia, F., and Jetten, A.M. (2007). The ubiquitin-interacting motif containing protein RAP80 interacts with BRCA1 and functions in DNA damage repair response. *Cancer Res.* 67, 6647–6656.
- You, Z., Chahwan, C., Bailis, J., Hunter, T., and Russell, P. (2005). ATM activation and its recruitment to damaged DNA require binding to the C terminus of Nbs1. *Mol. Cell. Biol.* 25, 5363–5379.